

Experimental Observation of Topological Disclination States in Lossy Electric Circuits

Jin Liu,^{1,*} Wei-Wu Jin,^{1,*} Zhao-Fan Cai,^{1,*} Xin Wang,² Yu-Ran Zhang,¹
Xiaomin Wei,¹ Wenbo Ju,^{1,†} Zhongmin Yang,^{1,3,4,‡} and Tao Liu^{1,§}

¹*School of Physics and Optoelectronics, South China University of Technology, Guangzhou 510640, China*

²*Institute of Theoretical Physics, School of Physics,
Xi'an Jiaotong University, Xi'an 710049, China*

³*Research Institute of Future Technology, South China Normal University, Guangzhou 510006, China*

⁴*State Key Laboratory of Luminescent Materials and Devices and Institute of Optical Communication Materials,
South China University of Technology, Guangzhou 510640, China*

(Dated: February 27, 2025)

Topological phase transitions can be remarkably induced purely by manipulating gain and loss mechanisms, offering a novel approach to engineering topological properties. Recent theoretical studies have revealed gain-loss-induced topological disclination states, along with the associated fractional charge trapped at the disclination sites. Here, we present the experimental demonstration of topological disclination states in a purely lossy electric circuit. By designing alternating lossy electric circuit networks that correspond to the disclination lattice, we observe a voltage response localized at the disclination sites and demonstrate the robustness of these states against disorder. Furthermore, we measure the charge distribution, confirming the presence of fractional charge at the disclination sites, which gives rise to the topological disclination states. Our experiment provides direct evidence of gain-loss-induced topological disclination states in electric circuits, opening new possibilities for applications in classical systems.

Introduction.—Over the past decade, topological phases of matter have revolutionized our understanding of quantum materials and wave dynamics, introducing a transformative paradigm in modern physics [1, 2]. Initially rooted in condensed matter systems [3–5], these phases are characterized by robust edge states and global topological invariants. Their influence has since expanded beyond electronic systems to photonics [6–8], acoustic and mechanical systems [9–12], and electric circuits [13–16]. These advances promise technological breakthroughs in robust signal transport, disorder-resistant devices, and novel quantum computing architectures [2, 17].

Recent developments have further extended topology to non-Hermitian systems, which provide a natural framework for describing open dynamical systems that exchange particles and energy with their surroundings [18–20]. The rapidly evolving field of non-Hermitian physics has uncovered a range of exotic phenomena absent in Hermitian counterparts [21–60]. These include exceptional points [61–63], the non-Hermitian skin effect [64–69], and unconventional bulk-boundary correspondence [64–67]. Notably, topological phase transitions can be induced purely by manipulating gain and loss mechanisms [70–74], enabling a novel approach to engineering topological properties. This highlights the profound interplay between dissipation and topology, paving the way for new phases of matter beyond conventional Hermitian frameworks.

Parallel to these developments, the study of topological crystalline insulators has demonstrated how crystalline symmetries, such as mirror and rotational symmetries, can stabilize distinct topological phases [75–77]. Unlike

conventional topological insulators, which are protected by internal symmetries like time-reversal, particle-hole, or chiral symmetry [5], topological crystalline insulators derive their robustness from the spatial symmetries of the crystal lattice. This leads to exotic boundary phenomena, such as hinge and corner states [78, 79], as well as unusual quantized electric responses, including fractional electric polarization and boundary-localized fractional charge [80–82], which are directly linked to the crystal's geometric structure.

A particularly intriguing aspect of topological crystalline insulators is their response to crystallographic defects, such as dislocations [83–87] and disclinations [81, 82, 88–91]. In particular, disclinations, which result from rotational misorientations in the lattice, serve as a unique platform for investigating the interplay between topology and symmetry breaking [81, 88]. In Hermitian cases, disclinations can trap fractional charge, providing a direct manifestation of bulk topology [81, 82, 88–91]. Despite significant progress in both non-Hermitian topology and topological disclination states, their intersection remains largely unexplored. Non-Hermitian topological crystalline insulators establish a novel framework where crystalline symmetries and non-Hermiticity intertwine, giving rise to exotic defect-bound states governed by gain-loss mechanisms. Recent theoretical studies predict the emergence of gain-loss-induced topological disclination states [92], providing a unique platform to explore non-Hermitian effects on symmetry-protected topological phases. However, experimental validation is still lacking, though promising realizations can be achieved by employing electric circuits [93–98].

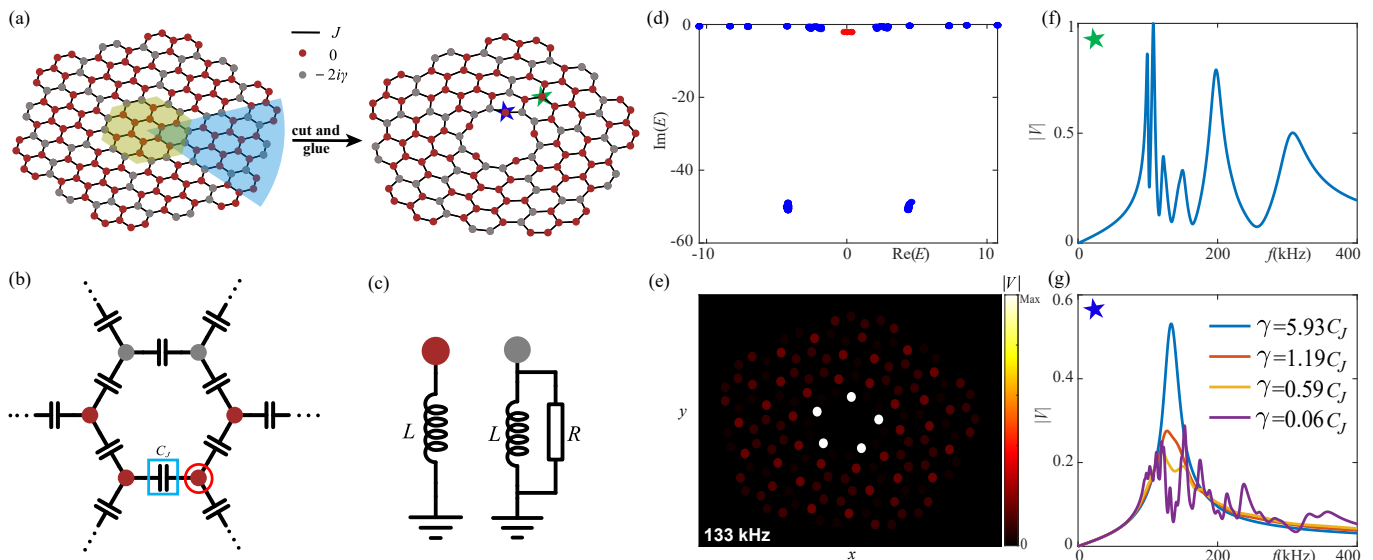


FIG. 1. (a) Schematic of a 2D non-Hermitian lattice with a disclination, created by cutting and gluing a pristine honeycomb lattice. The lattice sites represented by gray dots are dissipative, with a loss rate of -2γ , while the red sites are dissipationless. The nearest-neighbor hopping (black lines) is denoted by J . The green and blue stars mark the bulk site and disclination site, respectively. (b) Grounded components of the electric circuit for simulating the disclination lattice in (a), where the red and gray dots represent the disclination-lattice sites within a hexagonal structure. At each red site, the corresponding node is connected to three nearest-neighbor capacitors and one grounded inductor, as illustrated in panel (c). At each gray site, the node is connected to three nearest-neighbor capacitors, one grounded inductor and one grounded resistor [see panel (c)], where the resistor is used to introduce onsite loss. (d) Simulated complex eigenvalue E , where the red dots represent five disclination states. (e) The corresponding simulated voltage distribution $|V(x, y)|$ by exciting each circuit node using alternating voltage with the resonance frequency of $f_0 = 133$ kHz. Simulated voltage response $|V|$ (f) at a bulk site (green star) and (g) at a disclination site (blue star) for different loss γ as a function of excitation frequency f . Simulation parameters are $C_J = 100$ nF, $R = 1 \Omega$, and $L = 4.7 \mu\text{H}$.

In this work, we report the experimental observation of non-Hermitian topological disclination states in lossy electric circuits. Using the tight-binding model of the topological disclination lattice [92], we simulate and design corresponding electric circuit networks. The gain and loss mechanisms are controlled through alternating resistors, which act as the alternating loss. By exciting each circuit node with an alternating voltage at the resonance frequency, we measure the voltage response and observe in-gap states that become localized at the disclination sites in the presence of strong loss. The robustness against disorder is verified by measuring the voltage response in a circuit where random resistors are applied at each node. Furthermore, we measure the charge distribution, confirming the fractional charge trapped at the disclination sites, which is integer for a lossless circuit. Our observations provide direct evidence of topological disclination states induced by gain-loss effects.

Setup.—We begin by introducing an electric circuit model designed to simulate a non-Hermitian lattice with a disclination, as shown in Fig. 1(a). This model supports topological disclination states associated with a fractional charge of $1/2$ [92]. The disclination lattice is created by cutting and reassembling a pristine

honeycomb lattice [see Fig. 1(a)]. The lattice sites represented by gray dots are dissipative, with a loss rate of -2γ , while the red sites are dissipationless. The nearest-neighbor hopping (black lines) is denoted by J .

This disclination lattice can be effectively implemented using an electrical circuit network. Figures 1(b,c) show the grounded components of the electric circuit designed to simulate the disclination lattice depicted in Fig. 1(a), with the red and gray dots representing the disclination-lattice sites within the hexagonal structure. At each red site, the corresponding node is connected to three nearest-neighbor capacitors with capacitance C_J and one grounded inductor with inductance L , as shown in Fig. 1(c). At each gray site, the node is connected to three nearest-neighbor capacitors with capacitance C_J , one grounded inductor with inductance L and one grounded resistor with resistance R (see Fig. 1(c)), where the resistor introduces onsite loss.

Using Kirchhoff's laws [14], the disclination-lattice model in Fig. 1(a) is represented by the circuit Laplacian $J(\omega) = \mathcal{H}_{\text{cir}} - E \sum_n a_n^\dagger a_n$ of the circuit in Fig. 1(b,c). Here, $E = 3C_J - 1/(\omega^2 L)$, and \mathcal{H}_{cir} is analogous to the Hamiltonian of the disclination model. The Laplacian relates the grounded-voltage vector \mathbf{V} to the input current vector \mathbf{I} through the equation $\mathbf{I}(\omega) =$

$J(\omega)\mathbf{V}(\omega)$. For the zero input current, the circuit equation is expressed as

$$\mathcal{H}_{\text{cir}}\mathbf{V} = \left(3C_J - \frac{1}{\omega^2 L}\right)\mathbf{V}, \quad (1)$$

with

$$\mathcal{H}_{\text{cir}} = -i \sum_n \gamma_n a_n^\dagger a_n + C_J \sum_{\langle nn' \rangle} a_n^\dagger a_{n'} \quad (2)$$

where $\langle \dots \rangle$ denotes the nearest-neighbor hopping, γ_n represents the onsite loss rate with $\gamma_n = 0$ at the red node and $\gamma_n = 1/(\omega R)$ at the gray sites. In this paper, otherwise specifically, we use the following experimental parameters: $C_J = 100$ nF, $R = 1$ Ω , and $L = 4.7$ μH , where the resonant frequency of the circuit is calculated as $f_0 = 1/(2\pi\sqrt{3LC_J}) \simeq 133$ kHz, corresponding to $E = 0$. Note that, as shown in Eqs. (1) and (2), the circuit Laplacian $J(\omega)$ reflects the Hamiltonian matrix of the tight-binding lattice at the resonance frequency $\omega = \omega_0 = 2\pi f_0$.

Figure 1(d) shows the simulated complex eigenvalue E . The in-gap states (red dots) correspond to the topological disclination states for $\gamma = 5.93C_J$ at gray sites. The corresponding simulated voltage distribution $|V(x, y)|$, obtained by exciting each circuit node with an alternating voltage at a frequency of $f = 133$ kHz, is shown in Fig. 1(e), where the in-gap states are well localized at disclination states. Note that the bulk sites and disclination sites show distinct voltage response, as shown in Fig. 1(f,g). This allows us to resolve the disclination states by applying an alternating voltage at the resonance frequency ω_0 . In addition, the well-resolved voltage response at the disclination site occurs for a large loss rate γ , where the peak resonant frequency is around $f_0 = 133$ kHz for $\gamma = 5.93C_J$ at gray sites [see Fig. 1(g)].

Experimental Results.—In order to experimentally verify gain-loss-induced topological disclination states and their associated fractional charges [92], we fabricate electric circuits, with their photographs shown in Fig. 2(a,b), where the lattice site and nearest-neighbor reciprocal hopping are highlighted by red and yellow boxes, respectively. We measure the voltage response, $|V|$, of this circuit when excited at the disclination site as a function of driving frequency f for different loss rates γ at gray sites [see Fig. 2(c)]. The measured resonant peak occurs around 134 kHz, which is in close agreement with the theoretical value shown in Fig. 1(g). Further details about the simulation and measurement methods are provided in the Supplemental Material (SM) in Ref. [99].

To experimentally measure the topological disclination states, we excite each circuit node with an alternating voltage at a frequency of $f = 134$ kHz, which resonates with the disclination states. We measure the responded voltage distribution $|V(x, y)|$ for different loss rates γ at

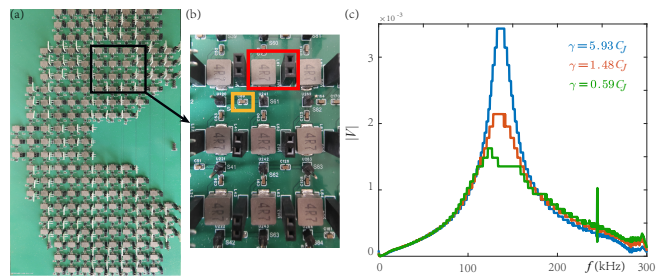


FIG. 2. (a) Photograph of the printed circuit board fabricated based on the schematics in Fig. 1(b,c). (b) Enlarged view of the printed circuit board, highlighting lattice sites and nearest-neighbor reciprocal hopping with red and yellow boxes, respectively. (c) Measured voltage response $|V|$ of the circuit excited at the disclination site as a function of driving frequency f for different loss rate γ at gray sites. The measured resonant peak is around 134 kHz.

gray sites, as shown in Fig. 3. The disclination states cannot be clearly resolved for the weak loss rate for $\gamma = 0.59C_J$, as shown in Fig. 3(a), which is consistent with the simulated voltage response in Fig. 1(g) under weak resonance at 134 kHz. As the loss rate increases, a well-resolved disclination distribution is observed for $\gamma = 5.93C_J$, as shown in Fig. 3(c).

To assess the robustness of topological disclination states, we introduce a random onsite disorder potential by assigning a random resistor to each node. The random resistor values are uniformly drawn from the range $[-0.2\gamma, 0.2\gamma]$. As shown in Fig. 4, we measure voltage distribution $|V(x, y)|$ by exciting each circuit node with an alternating voltage at a frequency of $f = 134$ kHz for $\gamma = 5.93C_J$ at gray sites.

In Hermitian topological lattice systems, disclinations act as defects that trap fractional charges, directly reflecting the bulk topology [81, 82, 88–91]. Interestingly, theoretical studies have shown that non-Hermitian topological disclination lattices exhibit a similar phenomenon, with fractional charge trapping serving as a hallmark of their topological nature [92].

We now move on to the experimental verification of fractional charge distribution at the disclination sites.

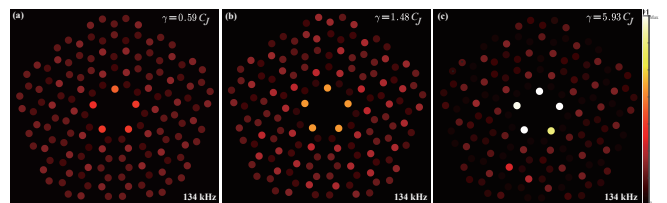


FIG. 3. Experimental results of the measured voltage distribution $|V(x, y)|$, are obtained by exciting each circuit node with an alternating voltage at a frequency of $f = 134$ kHz for different loss rates γ at gray sites: (a) $\gamma = 0.59C_J$, (b) $\gamma = 1.48C_J$, and (c) $\gamma = 5.93C_J$.

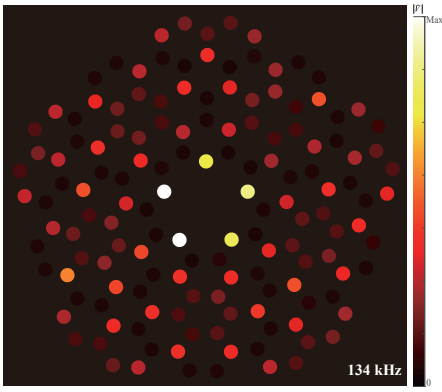


FIG. 4. Experimental results of the measured voltage distribution, $|V(x, y)|$, are obtained by exciting each circuit node with an alternating voltage at the frequency of $f = 134$ kHz for $\gamma = 5.93C_J$ at gray sites. The system is subjected to an onsite random potential by assigning a random resistor, with its value chosen from the range $[-0.2\gamma, 0.2\gamma]$, at each node. The results are averaged over 10 realizations of the disorder.

One approach to identifying disclination charge is by analyzing the local density of states [80, 82, 90, 92, 100]. This can be determined using the Laplacian matrix $J(\omega)$ of the circuit at the resonance frequency $\omega = \omega_0$. The Laplacian matrix $J(\omega_0)$ is reconstructed by measuring the voltage response at all lattice sites. By inverting $J(\omega_0)$, the circuit Hamiltonian \mathcal{H}_{cir} is obtained, encapsulating the key physical insights of the disclination model. Finally, diagonalizing \mathcal{H}_{cir} yields the left and right eigenvectors of the circuit, with

$$\mathcal{H}_{\text{cir}} |\psi_n^R\rangle = E |\psi_n^R\rangle, \quad \mathcal{H}_{\text{cir}}^\dagger |\psi_n^L\rangle = E^* |\psi_n^L\rangle, \quad (3)$$

where $|\psi_n^R\rangle$ and $|\psi_n^L\rangle$ denote the n th right and left eigenvector of the circuit Hamiltonian \mathcal{H}_{cir} , with $\langle \psi_n^R | \psi_{n'}^L \rangle = \delta_{nn'}$.

The charge Q_d in a specific region of the circuit can be determined as

$$Q_d = \sum_l \sum_n |\langle \psi_n^L | l \rangle \langle l | \psi_n^R \rangle| \pmod{1}, \quad (4)$$

where l denotes the indices of the lattice sites, while the index n represents the eigenstate corresponding to the specific eigenvalue. For bulk sites, l is taken within a unit cell. For studying disclination sites, l is taken within a unit cell plus the nearest neighboring disclination site. The index n is taken over all occupied states.

Figure 5(a,b) show the measured charge distribution Q_d for the lossy disclination lattice with $\gamma = 5.93C_J$ at gray sites. In the bulk region at each unit cell is approximately $Q_d \simeq 0$ [see Fig. 5(a)]. However, at the disclination site, the charge becomes fractional with $Q_d \simeq 0.5$ [see Fig. 5(b)]. The experimental results closely align with the theoretical ones (see details in

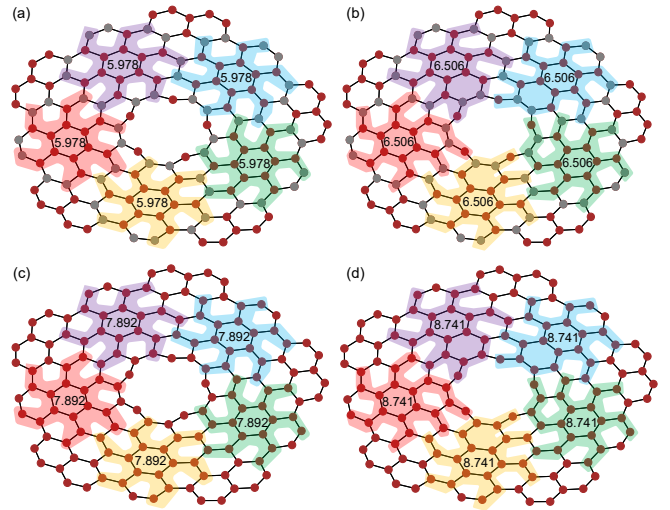


FIG. 5. Charge distribution Q_d (a,b) for the lossy disclination lattice with $\gamma = 5.93C_J$ at gray sites, and (c,d) for the lossless disclination lattice with $\gamma = 0$ at all sites. The charge is calculated (a, c) with a unit cell, and (b, d) with a unit cell plus one disclination site.

SM [99]). In contrast, for the lossless circuit lattice, the charge in the bulk region at each unit cell and disclination site is approximately $Q_d \simeq 0.9$ and $Q_d \simeq 0.7$, as shown in Fig. 5(c,d). The half-valued charge verifies the topological nature of the localized disclination states.

Conclusion.—We design and simulate the electric-circuit lattice of a tight-binding model for a topological disclination lattice. The circuit is purely dissipative, with alternating resistors introduced. We excite the circuit nodes using an alternating voltage and measure the voltage response. Well-localized disclination states are observed, and their robustness against disorder is demonstrated. Furthermore, we measure the charges at both bulk and disclination sites, finding integer charges at bulk unit cells and fractional charges at disclination sites, which highlights the topological nature of the disclination states. Our electric-circuit experiments directly verify the gain-loss-induced topological disclination sites, paving the way for the exploration of novel dissipative topological phases in classical systems and potential topological applications.

T.L. acknowledges the support from the National Natural Science Foundation of China (Grant No. 12274142), the Fundamental Research Funds for the Central Universities (Grant No. 2023ZYGXZR020), Introduced Innovative Team Project of Guangdong Pearl River Talents Program (Grant No. 2021ZT09Z109), and the Startup Grant of South China University of Technology (Grant No. 20210012). XW is supported by the National Natural Science Foundation of China (NSFC) (No. 12174303). Y.R.Z. thanks the support from the National Natural Science Foundation of China (Grant No. 12475017), Natural Science Foundation of

Guangdong Province (Grant No. 2024A1515010398), and the Startup Grant of South China University of Technology (Grant No. 20240061). W.J. thanks the support from the National Natural Science Foundation of China (No. U21A2093) and Introduced Innovative Team Project of Guangdong Pearl River Talents Program (Grant No. 2021ZT09Z109). F.N. is supported in part by: Nippon Telegraph and Telephone Corporation (NTT) Research, the Japan Science and Technology Agency (JST) [via the CREST Quantum Frontiers program Grant No. JPMJCR24I2, the Quantum Leap Flagship Program (Q-LEAP), and the Moonshot R&D Grant Number JPMJMS2061], and the Office of Naval Research (ONR) Global (via Grant No. N62909-23-1-2074).

Note Added.—Upon finalizing this draft, we became aware of a recent preprint [101] that also reports topological disclination states in gain and loss circuits.

* These authors contributed equally

† E-mail: wjuphy@scut.edu.cn

‡ E-mail: yangzm@scut.edu.cn

§ E-mail: liutao0716@scut.edu.cn

- [1] A. B. Khanikaev and G. Shvets, “Two-dimensional topological photonics,” *Nat. Photon.* **11**, 763 (2017).
- [2] O. Breunig and Y. Ando, “Opportunities in topological insulator devices,” *Nat. Rev. Phys.* **4**, 184 (2021).
- [3] M. Z. Hasan and C. L. Kane, “Colloquium: Topological insulators,” *Rev. Mod. Phys.* **82**, 3045 (2010).
- [4] X.-L. Qi and S.-C. Zhang, “Topological insulators and superconductors,” *Rev. Mod. Phys.* **83**, 1057 (2011).
- [5] C.-K. Chiu, J. C. Y. Teo, A. P. Schnyder, and S. Ryu, “Classification of topological quantum matter with symmetries,” *Rev. Mod. Phys.* **88**, 035005 (2016).
- [6] L. Lu, J. D. Joannopoulos, and M. Soljačić, “Topological photonics,” *Nat. Photonics* **8**, 821 (2014).
- [7] T. Ozawa, H. M. Price, A. Amo, N. Goldman, M. Hafezi, L. Lu, M. C. Rechtsman, D. Schuster, J. Simon, O. Zilberberg, and I. Carusotto, “Topological photonics,” *Rev. Mod. Phys.* **91**, 015006 (2019).
- [8] C. Leefmans, A. Dutt, J. Williams, L. Yuan, M. Parto, F. Nori, S. Fan, and A. Marandi, “Topological dissipation in a time-multiplexed photonic resonator network,” *Nat. Phys.* **18**, 442 (2022).
- [9] S. D. Huber, “Topological mechanics,” *Nat. Phys.* **12**, 621 (2016).
- [10] D. Z. Rocklin, S. Zhou, K. Sun, and X. Mao, “Transformable topological mechanical metamaterials,” *Nat. Commun.* **8**, 14201 (2017).
- [11] X. Li, F. and Huang, J. Lu, J. Ma, and Z. Liu, “Weyl points and Fermi arcs in a chiral phononic crystal,” *Nat. Phys.* **14**, 30 (2017).
- [12] G. Ma, M. Xiao, and C. T. Chan, “Topological phases in acoustic and mechanical systems,” *Nat. Rev. Phys.* **1**, 281 (2019).
- [13] S. Imhof, C. Berger, F. Bayer, J. Brehm, L. W. Molenkamp, T. Kiessling, F. Schindler, C. H. Lee, M. Greiter, T. Neupert, and R. Thomale, “Topoelectrical-circuit realization of topological corner modes,” *Nat. Phys.* **14**, 925 (2018).
- [14] C. H. Lee, S. Imhof, C. Berger, F. Bayer, J. Brehm, L. W. Molenkamp, T. Kiessling, and R. Thomale, “Topoelectrical Circuits,” *Commun. Phys.* **1** (2018), [10.1038/s42005-018-0035-2](https://doi.org/10.1038/s42005-018-0035-2).
- [15] H. Yang, L. Song, Y. Cao, and P. Yan, “Circuit realization of topological physics,” *Phys. Rep.* **1093**, 1 (2024).
- [16] W. Zhang, W. Cao, L. Qian, H. Yuan, and X. Zhang, “Topoelectrical space-time circuits,” *Nat. Commun.* **16**, 198 (2025).
- [17] N. H. Nickerson, Y. Li, and S. C. Benjamin, “Topological quantum computing with a very noisy network and local error rates approaching one percent,” *Nat. Commun.* **4**, 1756 (2013).
- [18] C. M. Bender, “Making sense of non-Hermitian Hamiltonians,” *Rep. Prog. Phys.* **70**, 947 (2007).
- [19] Ramy El-Ganainy, Konstantinos G. Makris, Mercedeh Khajavikhan, Ziad H. Musslimani, Stefan Rotter, and Demetrios N. Christodoulides, “Non-Hermitian physics and PT symmetry,” *Nat. Phys.* **14**, 11 (2018).
- [20] Y. Ashida, Z. Gong, and M. Ueda, “Non-Hermitian physics,” *Adv. Phys.* **69**, 249 (2020).
- [21] F. Monifi, J. Zhang, Ş. K. Özdemir, B. Peng, Y.-x. Liu, F. Bo, F. Nori, and L. Yang, “Optomechanically induced stochastic resonance and chaos transfer between optical fields,” *Nat. Photon.* **10**, 399 (2016).
- [22] J. Zhang, B. Peng, Ş. K. Özdemir, K. Pichler, D. O. Krimer, G. Zhao, F. Nori, Y.-x. Liu, S. Rotter, and L. Yang, “A phonon laser operating at an exceptional point,” *Nat. Photon.* **12**, 479 (2018).
- [23] Y. Xu, S. T. Wang, and L. M. Duan, “Weyl exceptional rings in a three-dimensional dissipative cold atomic gas,” *Phys. Rev. Lett.* **118**, 045701 (2017).
- [24] Z. Gong, Y. Ashida, K. Kawabata, K. Takasan, S. Higashikawa, and M. Ueda, “Topological phases of non-Hermitian systems,” *Phys. Rev. X* **8**, 031079 (2018).
- [25] B. Peng, S. K. Özdemir, S. Rotter, H. Yilmaz, M. Liertzer, F. Monifi, C. M. Bender, F. Nori, and L. Yang, “Loss-induced suppression and revival of lasing,” *Science* **346**, 328 (2014).
- [26] R. El-Ganainy, K. G. Makris, M. Khajavikhan, Z. H. Musslimani, S. Rotter, and D. N. Christodoulides, “Non-Hermitian physics and PT symmetry,” *Nat. Phys.* **14**, 11 (2018).
- [27] F. Song, S. Yao, and Z. Wang, “Non-Hermitian skin effect and chiral damping in open quantum systems,” *Phys. Rev. Lett.* **123**, 170401 (2019).
- [28] J. Y. Lee, J. Ahn, H. Zhou, and A. Vishwanath, “Topological correspondence between Hermitian and non-Hermitian systems: Anomalous dynamics,” *Phys. Rev. Lett.* **123**, 206404 (2019).
- [29] K. Kawabata, T. Bessho, and M. Sato, “Classification of exceptional points and non-Hermitian topological semimetals,” *Phys. Rev. Lett.* **123**, 066405 (2019).
- [30] L. Li, C. H. Lee, and J. Gong, “Topological switch for non-Hermitian skin effect in cold-atom systems with loss,” *Phys. Rev. Lett.* **124**, 250402 (2020).
- [31] L. Li, C. H. Lee, S. Mu, and J. Gong, “Critical non-Hermitian skin effect,” *Nat. Commun.* **11**, 5491 (2020).
- [32] N. Okuma, K. Kawabata, K. Shiozaki, and M. Sato, “Topological origin of non-Hermitian skin effects,”

- Phys. Rev. Lett.* **124**, 086801 (2020).
- [33] Y. Yi and Z. Yang, “Non-Hermitian skin modes induced by on-site dissipations and chiral tunneling effect,” *Phys. Rev. Lett.* **125**, 186802 (2020).
- [34] Z. Y. Ge, Y. R. Zhang, T. Liu, S. W. Li, H. Fan, and F. Nori, “Topological band theory for non-Hermitian systems from the Dirac equation,” *Phys. Rev. B* **100**, 054105 (2019).
- [35] H. Zhou and J. Y. Lee, “Periodic table for topological bands with non-Hermitian symmetries,” *Phys. Rev. B* **99**, 235112 (2019).
- [36] H. Zhao, X. Qiao, T. Wu, B. Midya, S. Longhi, and L. Feng, “Non-Hermitian topological light steering,” *Science* **365**, 1163 (2019).
- [37] K. Kawabata, K. Shiozaki, M. Ueda, and M. Sato, “Symmetry and topology in non-Hermitian physics,” *Phys. Rev. X* **9**, 041015 (2019).
- [38] D. S. Borgnia, A. J. Kruchkov, and R.-J. Slager, “Non-Hermitian boundary modes and topology,” *Phys. Rev. Lett.* **124**, 056802 (2020).
- [39] T. Liu, J. J. He, T. Yoshida, Z.-L. Xiang, and F. Nori, “Non-Hermitian topological Mott insulators in one-dimensional fermionic superlattices,” *Phys. Rev. B* **102**, 235151 (2020).
- [40] K. Y. Bliokh, D. Leykam, M. Lein, and F. Nori, “Topological non-Hermitian origin of surface Maxwell waves,” *Nat. Comm.* **10**, 580 (2019).
- [41] K. Yokomizo and S. Murakami, “Scaling rule for the critical non-Hermitian skin effect,” *Phys. Rev. B* **104**, 165117 (2021).
- [42] H. Jiang and C. H. Lee, “Dimensional transmutation from non-Hermiticity,” *Phys. Rev. Lett.* **131**, 076401 (2023).
- [43] T. Liu, J. J. He, Z. Yang, and F. Nori, “Higher-order Weyl-exceptional-ring semimetals,” *Phys. Rev. Lett.* **127**, 196801 (2021).
- [44] E. J. Bergholtz, J. C. Budich, and F. K. Kunst, “Exceptional topology of non-Hermitian systems,” *Rev. Mod. Phys.* **93**, 015005 (2021).
- [45] Y. Li, C. Liang, C. Wang, C. Lu, and Y.-C. Liu, “Gain-loss-induced hybrid skin-topological effect,” *Phys. Rev. Lett.* **128**, 223903 (2022).
- [46] Q. Wang, C. Zhu, X. Zheng, H. Xue, B. Zhang, and Y. D. Chong, “Continuum of bound states in a non-Hermitian model,” *Phys. Rev. Lett.* **130**, 103602 (2023).
- [47] K. Zhang, Z. Yang, and C. Fang, “Universal non-Hermitian skin effect in two and higher dimensions,” *Nat. Commun.* **13** (2022), 10.1038/s41467-022-30161-6.
- [48] M. Parto, C. Leefmans, J. Williams, F. Nori, and A. Marandi, “Non-Abelian effects in dissipative photonic topological lattices,” *Nat. Comm.* **14**, 1440 (2023).
- [49] Z. Ren, D. Liu, E. Zhao, C. He, K. K. Pak, J. Li, and G.-B. Jo, “Chiral control of quantum states in non-Hermitian spin-orbit-coupled fermions,” *Nat. Phys.* **18**, 385 (2022).
- [50] K. Kawabata, T. Numasawa, and S. Ryu, “Entanglement phase transition induced by the non-Hermitian skin effect,” *Phys. Rev. X* **13**, 021007 (2023).
- [51] C.-A. Li, B. Trauzettel, T. Neupert, and S.-B. Zhang, “Enhancement of second-order non-Hermitian skin effect by magnetic fields,” *Phys. Rev. Lett.* **131**, 116601 (2023).
- [52] J. Liu, Z.-F. Cai, T. Liu, and Z. Yang, “Reentrant non-Hermitian skin effect in coupled non-Hermitian and Hermitian chains with correlated disorder,” [arXiv:2311.03777](https://arxiv.org/abs/2311.03777) (2023).
- [53] Z.-F. Cai, T. Liu, and Z. Yang, “Non-Hermitian skin effect in periodically driven dissipative ultracold atoms,” *Phys. Rev. A* **109**, 063329 (2024).
- [54] X. Li, J. Liu, and T. Liu, “Localization-delocalization transitions in non-Hermitian Aharonov-Bohm cages,” *Front. Phys.* **19**, 33211 (2024).
- [55] H.-Y. Wang, F. Song, and Z. Wang, “Amoeba formulation of non-Bloch band theory in arbitrary dimensions,” *Phys. Rev. X* **14**, 021011 (2024).
- [56] K. Zhang, C. Fang, and Z. Yang, “Dynamical degeneracy splitting and directional invisibility in non-Hermitian systems,” *Phys. Rev. Lett.* **131**, 036402 (2023).
- [57] Y.-M. Hu, H.-Y. Wang, Z. Wang, and F. Song, “Geometric origin of non-Bloch \mathcal{PT} symmetry breaking,” *Phys. Rev. Lett.* **132**, 050402 (2024).
- [58] C. R. Leefmans, M. Parto, J. Williams, G. H. Y. Li, A. Dutt, F. Nori, and A. Marandi, “Topological temporally mode-locked laser,” *Nat. Phys.* **20**, 852 (2024).
- [59] M. Yang and C. H. Lee, “Percolation-induced \mathcal{PT} symmetry breaking,” *Phys. Rev. Lett.* **133**, 136602 (2024).
- [60] Z.-F. Cai, Y.-C. Wang, and T. Liu, “Nonlinearity-driven morphing and control of topological modes in non-Hermitian systems,” [arXiv:2411.10398](https://arxiv.org/abs/2411.10398) (2024).
- [61] Ş. K. Özdemir, S. Rotter, F. Nori, and L. Yang, “Parity-time symmetry and exceptional points in photonics,” *Nat. Mater.* **18**, 783 (2019).
- [62] K. Ding, C. Fang, and G. Ma, “Non-Hermitian topology and exceptional-point geometries,” *Nat. Rev. Phys.* **4**, 745 (2022).
- [63] A. Li, H. Wei, M. Cotrufo, W. Chen, S. Mann, X. Ni, B. Xu, J. Chen, J. Wang, S. Fan, C.-W. Qiu, A. Alù, and L. Chen, “Exceptional points and non-Hermitian photonics at the nanoscale,” *Nat. Nano.* **18**, 706 (2023).
- [64] S. Yao and Z. Wang, “Edge states and topological invariants of non-Hermitian systems,” *Phys. Rev. Lett.* **121**, 086803 (2018).
- [65] K. Zhang, Z. Yang, and C. Fang, “Correspondence between winding numbers and skin modes in non-Hermitian systems,” *Phys. Rev. Lett.* **125**, 126402 (2020).
- [66] K. Yokomizo and S. Murakami, “Non-Bloch band theory of non-Hermitian systems,” *Phys. Rev. Lett.* **123**, 066404 (2019).
- [67] S. Yao, F. Song, and Z. Wang, “Non-Hermitian Chern bands,” *Phys. Rev. Lett.* **121**, 136802 (2018).
- [68] F. K. Kunst, E. Edvardsson, J. C. Budich, and E. J. Bergholtz, “Biorthogonal bulk-boundary correspondence in non-Hermitian systems,” *Phys. Rev. Lett.* **121**, 026808 (2018).
- [69] T. Liu, Y.-R. Zhang, Q. Ai, Z. Gong, K. Kawabata, M. Ueda, and F. Nori, “Second-order topological phases in non-Hermitian systems,” *Phys. Rev. Lett.* **122**, 076801 (2019).
- [70] K. Takata and M. Notomi, “Photonic topological insulating phase induced solely by gain and loss,” *Phys. Rev. Lett.* **121**, 213902 (2018).
- [71] X.-W. Luo and C. Zhang, “Higher-order topological

- corner states induced by gain and loss,” *Phys. Rev. Lett.* **123**, 073601 (2019).
- [72] S. Liu, S. Ma, C. Yang, L. Zhang, W. Gao, Y. J. Xiang, T. J. Cui, and S. Zhang, “Gain- and loss-induced topological insulating phase in a non-Hermitian electrical circuit,” *Phys. Rev. Appl.* **13**, 014047 (2020).
- [73] H. Gao, H. Xue, Z. Gu, T. Liu, J. Zhu, and B. Zhang, “Non-Hermitian route to higher-order topology in an acoustic crystal,” *Nat. Commun.* **12**, 1888 (2021).
- [74] H. T. Teo, H. Xue, and B. Zhang, “Topological phase transition induced by gain and loss in a photonic Chern insulator,” *Phys. Rev. A* **105**, 053510 (2022).
- [75] L. Fu, “Topological crystalline insulators,” *Phys. Rev. Lett.* **106**, 106802 (2011).
- [76] F. Tang, H. C. Po, A. Vishwanath, and X. Wan, “Comprehensive search for topological materials using symmetry indicators,” *Nature* **566**, 486 (2019).
- [77] B. J. Wieder, B. Bradlyn, J. Cano, Z. Wang, M. G. Vergniory, L. Elcoro, A. A. Soluyanov, C. Felser, T. Neupert, N. Regnault, and B. A. Bernevig, “Topological materials discovery from crystal symmetry,” *Nat. Rev. Mater.* **7**, 196 (2021).
- [78] W. A. Benalcazar, B. A. Bernevig, and T. L. Hughes, “Electric multipole moments, topological multipole moment pumping, and chiral hinge states in crystalline insulators,” *Phys. Rev. B* **96**, 245115 (2017).
- [79] W. A. Benalcazar, B. A. Bernevig, and T. L. Hughes, “Quantized electric multipole insulators,” *Science* **357**, 61 (2017).
- [80] W. A. Benalcazar, T. Li, and T. L. Hughes, “Quantization of fractional corner charge in C_n -symmetric higher-order topological crystalline insulators,” *Phys. Rev. B* **99**, 245151 (2019).
- [81] T. Li, P. Zhu, W. A. Benalcazar, and T. L. Hughes, “Fractional disclination charge in two-dimensional C_n -symmetric topological crystalline insulators,” *Phys. Rev. B* **101**, 115115 (2020).
- [82] C. W. Peterson, T. Li, W. Jiang, T. L. Hughes, and G. Bahl, “Trapped fractional charges at bulk defects in topological insulators,” *Nature* **589**, 376 (2021).
- [83] Y. Ran, Y. Zhang, and A. Vishwanath, “One-dimensional topologically protected modes in topological insulators with lattice dislocations,” *Nat. Phys.* **5**, 298 (2009).
- [84] G. van Miert and C. Ortix, “Dislocation charges reveal two-dimensional topological crystalline invariants,” *Phys. Rev. B* **97**, 201111 (2018).
- [85] F.-F. Li, H.-X. Wang, Z. Xiong, Q. Lou, P. Chen, R.-X. Wu, Y. Poo, J.-H. Jiang, and S. John, “Topological light-trapping on a dislocation,” *Nat. Commun.* **9**, 2462 (2018).
- [86] A. K. Nayak, J. Reiner, R. Queiroz, H. Fu, C. Shekhar, B. Yan, C. Felser, N. Avraham, and H. Beidenkopf, “Resolving the topological classification of Bismuth with topological defects,” *Sc. Adv.* **5**, eaax6996 (2019).
- [87] B. Roy and V. Juričić, “Dislocation as a bulk probe of higher-order topological insulators,” *Phys. Rev. Res.* **3**, 033107 (2021).
- [88] W. A. Benalcazar, J. C. Y. Teo, and T. L. Hughes, “Classification of two-dimensional topological crystalline superconductors and Majorana bound states at disclinations,” *Phys. Rev. B* **89**, 224503 (2014).
- [89] Q. Wang, H. Xue, B. Zhang, and Y. D. Chong, “Observation of protected photonic edge states induced by real-space topological lattice defects,” *Phys. Rev. Lett.* **124**, 243602 (2020).
- [90] Y. Liu, S. Leung, F.-F. Li, Z.-K. Lin, X. Tao, Yin Poo, and J.-H. Jiang, “Bulk–disclination correspondence in topological crystalline insulators,” *Nature* **589**, 381 (2021).
- [91] M. Geier, I. C. Fulga, and A. Lau, “Bulk-boundary-defect correspondence at disclinations in rotation-symmetric topological insulators and superconductors,” *SciPost Physics* **10**, 092 (2021).
- [92] R. Banerjee, S. Mandal, Y. Y. Terh, S. Lin, G.-G. Liu, B. Zhang, and Y. D. Chong, “Topological disclination states and charge fractionalization in a non-Hermitian lattice,” *Phys. Rev. Lett.* **133**, 233804 (2024).
- [93] Y. Choi, C. Hahn, J. W. Yoon, and S. H. Song, “Observation of an anti-PT-symmetric exceptional point and energy-difference conserving dynamics in electrical circuit resonators,” *Nat. Commun.* **9**, 2182 (2018).
- [94] T. Helbig, T. Hofmann, S. Imhof, M. Abdelghany, T. Kiessling, L. W. Molenkamp, C. H. Lee, A. Szameit, M. Greiter, and R. Thomale, “Generalized bulk–boundary correspondence in non-Hermitian topoelectrical circuits,” *Nat. Phys.* **16**, 747 (2020).
- [95] J. Wu, Z. Wang, Y. Biao, F. Fei, S. Zhang, Z. Yin, Y. Hu, Z. Song, T. Wu, F. Song, and R. Yu, “Non-Abelian gauge fields in circuit systems,” *Nat. Electron.* **5**, 635 (2022).
- [96] D. Zou, T. Chen, W. He, J. Bao, C. H. Lee, H. Sun, and X. Zhang, “Observation of hybrid higher-order skin-topological effect in non-Hermitian topoelectrical circuits,” *Nat. Commun.* **12**, 7201 (2021).
- [97] J. Hu, R.-Y. Zhang, Y. Wang, X. Ouyang, Y. Zhu, H. Jia, and C. T. Chan, “Non-Hermitian swallowtail catastrophe revealing transitions among diverse topological singularities,” *Nat. Phys.* **19**, 1098 (2023).
- [98] C.-X. Guo, L. Su, Y. Wang, L. Li, J. Wang, X. Ruan, Y. Du, D. Zheng, S. Chen, and H. Hu, “Scale-tailored localization and its observation in non-Hermitian electrical circuits,” *Nat. Commun.* **15**, 9120 (2024).
- [99] See Supplemental Material for detailed derivations.
- [100] M.-Y. Liu, F.-Y. Sun, Z.-G. Chen, Z. Wang, M.-H. Lu, and Y.-F. Chen, “Measurement of fractional charge in elastic plates with disclinations,” *Phys. Rev. Appl.* **22**, 014025 (2024).
- [101] R. Li, R. Banerjee, S. Mandal, Y. Long D. Li, T. Ma, J. Liu, Y. Chong G.-G. Liu, B. Zhang, and E.-P. Li, “Observation of non-Hermitian topological disclination states and charge fractionalization,” *arXiv:2502.04922* (2025).